A Body-Shadowing Model for Indoor Radio Communication Environments

Shuichi Obayashi, *Member, IEEE*, and Jens Zander, *Member, IEEE*

***Abstract*—Deterministic propagation prediction methods proposed for indoor radio are useful for estimating the average propagation loss in real environments, which usually have complicated geometries. On the other hand, these methods generally fail to accommodate human body shadowing, which is a significant propagation effect in indoor picocells. Several empirical models to describe body shadowing have been reported. However, to our knowledge, no appropriate model that can be used in combination with deterministic propagation prediction methods has been provided in the literature. In this paper, a new practical model is introduced, which provides a way to estimate body-shadowing effects deterministically with the existing ray-determination methods. The detailed procedure to combine our body-shadowing model with the ray-determination methods is described. Several examples are shown applying the procedure to a simple office layout.**

***Index Terms*—Indoor radio communication.**

I. Introduction

NUMEROUS propagation prediction methods have recently been proposed for indoor radio communications. The imaging method (e.g., [1], [2]) "ray tracing" (with origins in the computer graphics field) [3], [4] and the ray-splitting method [5] are typical examples. These methods have been designed mainly for system-planning purposes, e.g., for the selection of base-station locations in practical indoor environments. The main benefit of these deterministic prediction methods is that they successfully introduce an explicit dependence on the actual site geometry. This stands in contrast to some empirical models that are based on an abstract description of the sites (e.g., "factory with/without line-of-sight," "office with hard/soft partition," etc.).

Human body shadowing (Fig. 1) is a significant propagation effect in indoor picocells. In contrast to current outdoor cellular systems, the transmission power and the elevation of base stations is much lower in picocells. Thus, the propagation loss by body shadowing greatly affects the received signal strength even when considering a multipath environment where several rays contribute to the received power. In particular, this will be the case if the millimeter band (e.g., 60 GHz) is used instead of the UHF or L-bands, which are now widely used.

Some empirical models for body shadowing are available in the literature. Bultitude [6] assumed that the received signal amplitude has a Rician probability density function and determined the values of K (the ratio of the power in a steady signal to that in multipath components), which fit the measurement data taken in several buildings. Roberts *et al.* [7] proposed a two-state Rician model [7] to describe the bursty time varying characteristics caused by moving persons. They determined two different values of K for a measured result described in [6].

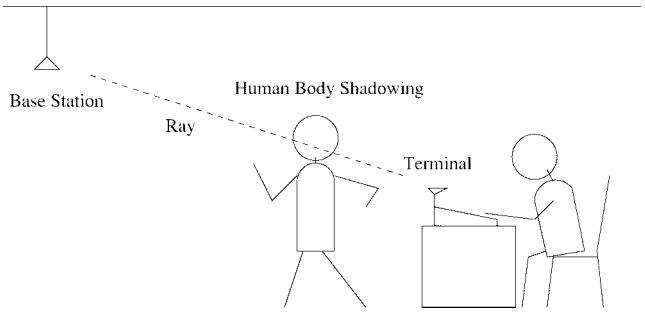

Fig. 1. Human body shadowing in indoor radio environment.

These empirical models, however, can introduce neither the dependency on actual relation in position among a base station, a terminal, walkways, walls, and other obstructions in a building, nor the influence of how frequent the "traffic" on each walkway is. Further, it is difficult to determine a certain value of K (or two certain values of K) for a certain indoor environment without a field measurement of the received signal strength under realistic conditions.

The only attempt in the literature to combine ray-determination methods to predict human body-shadowing effects is reported [8] in which continuous snapshot calculations are used for moving obstacles. This approach obviously requires lots of computational power and, thus, the size of the problem where this method can be used is limited.

In this report, we introduce a new and more practical method to estimate body-shadowing effects. This method is used with the existing ray-determination methods. We demonstrate that the proposed model can estimate the worst case in propagation loss due to the body shadowing, which is closely related to the outage rate of a communication link.

In Section II, the details of our body-shadowing model and the way to combine this model with the ray-determination methods such as the ray tracing and the imaging methods are described. In Section III, the model parameter selection based on several experimental results is described. In Section IV, we apply the body-shadowing model to a simple office layout and present some prediction results at 900 MHz and 60 GHz. In Section V, a measurement in 900-MHz band in a typical office

Manuscript received March 1, 1997; revised December 29, 1997.

S. Obayashi is with the Research and Development Center, Toshiba Corporation, Kawasaki 210, Japan.

J. Zander is with the Department of Signals, Sensors and Systems, Royal Institute of Technology (KTH), Stockholm, S-10044 Sweden.

Publisher Item Identifier S 0018-926X(98)04619-5.

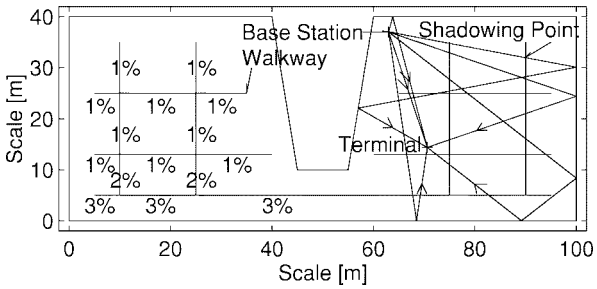

Fig. 2. Predicted rays, walkways, and shadowing points in an office.

is compared with the prediction based on the body-shadowing model.

II. Human Body-Shadowing Model

In this section, the steps to predict the probability density of the propagation loss due to the human body shadowing are shown. In this report, a two-dimensional ray determination will be used, but the same procedure can be applied to three-dimensional methods as well.

Step 0: Determine Influential Rays

In this step, we use one of the existing ray-determination methods mentioned in Section I. The method determines rays that depart from a base station and arrive at some given terminal position (Fig. 2). This kind of procedure usually determines a line-of-sight ray and rays that arrive at the receiving point via specular reflections, penetrations, diffractions and combinations of these phenomena. (Note that the contributions from rays penetrating walls can be neglected in Fig. 2.) If a ray is reflected by an object, a certain additional loss is added to the propagation loss. Penetration and diffraction phenomena also cause extra propagation losses. Thus, the propagation loss of each ray can be calculated. If a directional antenna is used for the base station and/or the terminal, the product of the directivities of the antennas and the propagation loss of each ray can be obtained. In the following discussion, the product of the directivity of the antennas and the propagation loss of ray i is simply denoted as L_i $(1 \leq i \leq N)$ where the number of the influential rays is N. In our calculation, an antenna with a radiation pattern (as shown in Fig. 3) is used at the base station. The antenna of the terminal is assumed to be omnidirectional.

Step 1: Obtain Discrete Probability Density of Local Average Propagation Loss

First, the paths along which people usually walk (*walkways*) are set on the plan of the given site (Fig. 2). The movement of people in a room is generally restricted by desks, tables, walls, partitions, and so on. Of course, there are many possible walkways (e.g., between the desks and chairs), but for the sake of simplicity, we will represent all these paths only by one walkway at the center of the free areas. Next, we define the *shadowing probability* of each walkway (again, see Fig. 2) by the probability that a person will be present at (cover) an arbitrary point on the walkway. As a walkway

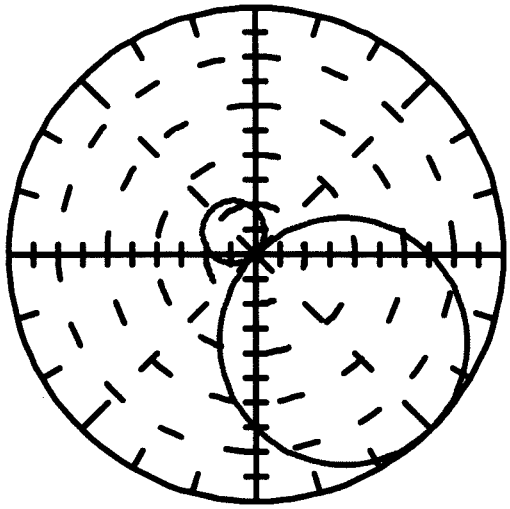

Fig. 3. Assumed field pattern of the directional antenna for the base station (Directivity: 6.8 dBi).

represents the possible walking paths in a certain space, persons walking on all of these walking paths should be included when determining this probability. Some straight walking paths may comprise several walkways with different shadowing probabilities, as can be seen at the bottom of Fig. 2. (In this figure, the shadowing probabilities are indicated on the walkways only in the left half of the map, but we set the probabilities symmetrically also in the right half.)

Second, we determine the intersections between rays calculated in the first step and the walkways, the *shadowing points*. Here we assume that a *shadowing event* (i.e., the event that a person shadows a ray) occurs at the shadowing points with the shadowing probability of the walkway where the shadowing point is located.

Since the shadowing events affecting rays passing the same walkway at almost the same point will be strongly correlated, we assume the following correlation model. We will assume that rays with shadowing points that are less than distance $d_{\rm th}$ (*threshold distance*) apart have identical shadowing events. Thus, the shadowing events at these shadowing points occur simultaneously. On the other hand, for shadowing points separated by more than the threshold distance, we assume that shadowing events are independent.

In our model, we assume that the propagation loss of a ray subject to one or multiple shadowing events on the ray increases by a constant $L_{\rm sh}$ [dB], denoted the *additional shadowing loss*.

Denote the event of shadowing at one or more shadowing points on ray i as S_i $(1 \leq i \leq N)$ and E_{il} denotes the event where lth point out of m shadowing points on ray i $(1 \leq l \leq m)$ is shadowed. In general

$$S_i = E_{i1} + E_{i2} + \cdots + E_{im}. \tag{1}$$

Note that the sign $+$ denotes the sum or union of events. (It can be written as $\cup$.) When the l_1th point and the l_2th point on ray i are close, $E_{il_1} = E_{il_2}$. Then $E_{il_1} + E_{il_2} = E_{il_1}$. Thus, only one of the two points is used in our calculation. If the l_1th

point on ray i and the l_2th point on ray j $(1 \le j \le N, j \ne i)$ are close, $E_{il_1} = E_{jl_2}$. Thus, S_i is not independent of S_j.

In a case where there are N rays reaching the receiver, there are 2^N combinations of shadowing/nonshadowing events for this set of rays. We will now obtain probabilities of these product events. Obviously, one of the product events is the event where none of the rays are shadowed $\overline{S_1}\,\overline{S_2}\cdots\overline{S_N}$. Another of these product event is the event where all of the rays are shadowed simultaneously $S_1S_2\cdots S_N$. We will now show how to calculate the probability of $S_1S_2\cdots S_N$ and that of $\overline{S_1}S_2\cdots S_{N-1}\overline{S_N}$ as examples. Other product event probabilities can be calculated in a similar manner. We assume that the shadowing event of ray j $(1 \le j \le M)$ is independent of the shadowing events of any other rays, i.e., ray k $(1 \le k \le N, k \ne j)$. M is the number of the independent events out of the N shadowing events and, thus, $0 \le M \le N$. Then the probabilities of the two product events are calculated by the following equation:

$$P(S_1, S_2, \cdots, S_N) = \underbrace{P(S_1)P(S_2)\cdots P(S_M)}_{\text{independent}}\underbrace{P(S_{M+1}, S_{M+2}, \cdots, S_N)}_{\text{not independent}} \tag{2}$$

$$P(\overline{S_1}, S_2, \cdots, S_{N-1}, \overline{S_N}) = \underbrace{P(\overline{S_1})P(S_2)\cdots P(S_M)}_{\text{independent}} \cdot \underbrace{P(S_{M+1}, S_{M+2}, \cdots, S_{N-1}, \overline{S_N})}_{\text{not independent}} \tag{3}$$

$P(\overline{S_j})$ and $P(S_j)$ $(1 \le j \le M)$ are simply calculated by

$$P(\overline{S_j}) = \prod_{l=1}^{m} (1 - P(E_{jl})) \tag{4}$$

$$P(S_j) = 1 - P(\overline{S_j}) \tag{5}$$

where E_{jl} is the event where the lth point out of m shadowing points on ray j $(1 \le l \le m)$ is shadowed. The detailed calculation of $P(S_{M+1}, S_{M+2}, \cdots, S_N)$ as well as $P(S_{M+1}, S_{M+2}, \cdots, S_{N-1}, \overline{S_N})$ is shown in the Appendix.

Finally, in this step, we calculate the local average propagation loss for each of the product events. The local average loss in a spatial range of several wavelengths around the observation point is calculated as the power sum (on a linear scale, not in decibels) of the losses of individual shadowed/nonshadowed incoming rays at the observation point [11]. For instance, if no rays are shadowed, the local average propagation loss is

$$L(\overline{S_1}, \overline{S_2}, \cdots, \overline{S_N}) = -10 \log \sum_{i=1}^{N} 10^{-L_i/10} \quad [\text{dB}] \tag{6}$$

when L_i [dB] $(1 \le i \le N)$ is the propagation loss of ray i (without shadowing) obtained in Step 0 and, at the event when all of the rays are shadowed simultaneously, the local average propagation loss is

$$L(S_1, S_2, \cdots, S_N) = -10 \log \sum_{i=1}^{N} 10^{-(L_i + L_{\text{sh}})/10} \quad [\text{dB}]. \tag{7}$$

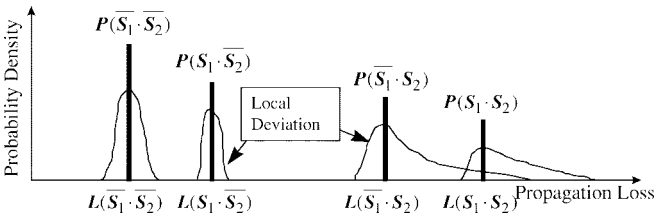

Fig. 4. Probability density of local average, local deviation by mutual phase relation among multipath, and total probability density of propagation loss.

We now obtain the discrete probability density function of the local average propagation loss in a spatial range of several wavelengths centered around the observation point given by $\{L(\overline{S_1}, \overline{S_2}, \cdots, \overline{S_N}), \cdots, L(S_1, S_2, \cdots, S_N)\}$ and $\{P(\overline{S_1}, \overline{S_2}, \cdots, \overline{S_N}), \cdots, P(S_1, S_2, \cdots, S_N)\}$ as shown in Fig. 4.

Step 2: Add Local Deviation by Multipath Phase Relation

The probability density of the local average propagation loss estimated at Step 1 can be quite useful in providing an overview of the human body-shadowing effects.

However, if we slightly change the position of a terminal receiving the signal from the base station, because of multipath effects, the receiving signal strength may change even in a static environment. This is due to the changing interrelations between the phase angles of different incoming rays [12], [13]. The variation in signal strength can be interpreted as the local deviation of the propagation loss within a small region (of the size of several wavelengths) centered around each observation point.

We will now attempt to obtain the probability densities of these local variations of the signal strength for individual product shadowing events (see Fig. 4) and weigh these densities by the discrete probabilities of the product events and add them up. In this way, it is possible to obtain a more realistic probability density in a spatial range of several wavelengths centered around the observation point. The precise probability density may then be used to estimate the spatial outage probability in the given geometry. The outage probability is one of the most important parameters in the design for an indoor radio communication system.

We can generally assume a uniformly distributed random phase relation among multipath components in the several wavelength range for the local averaging. Under this assumption, we now introduce the concept of *significant* rays. In our calculation, we define that the ith ray is *significant* if it is within 15 dB of the strongest ray in the product event, i.e., $L_i < L_{\min} + 15$ [dB], where $L_{\min}$ is the propagation loss of the strongest ray in the product event. (Note that the propagation loss *without shadowing* of the strongest among the influential rays, which is here denoted by L_a, is not always equal to $L_{\min}$.)

When only one ray is significant, we may assume that its amplitude variation is negligible.

For the case of two significant rays, we calculate the amplitude variation based on the assumption that the random

phases α, β of two sinusoids $A\cos(\omega_c t+\alpha), B\cos(\omega_c t+\beta)$ are independent and each of them is uniformly distributed from 0 to 2π. (The carrier frequency is denoted by ω_c and assume $A \geq B$.) If we denote the amplitude of the vector sum of the two sinusoids as R, the probability density function of R is [14]

$$p(R) = \begin{cases} \dfrac{2R}{\pi\sqrt{(2AB)^2-(A^2+B^2-R^2)^2}} \\ \qquad (A-B \leq R \leq A+B) \\ 0 \qquad (R < A-B \quad \text{or} \quad R > A+B). \end{cases} \tag{8}$$

When more than two rays are significant, we use an approximation yielding a Rice-distributed amplitude of the received signal [15]. The dominant component r_s in the Rice distribution is assumed to be the strongest ray in the product event and the mean power in the random components σ^2 is calculated as the power sum of the rest of the rays in the event. Though this approximation may overestimate the spread in amplitude, the computation time is reduced.

III. Model Parameter Selection

The model parameters $L_{\rm sh}$ (*additional shadowing loss*) and $d_{\rm th}$ (*threshold distance*) in Step 1 in Section II are inferred to depend on many factors, for example: carrier frequency, polarization, individual differences among shadowing persons, direction of the shadowing person relative to the ray (frontal or sideways), heights of antennas (base station, terminal), shadowing position on a ray (i.e., it is near or far from a base station or a terminal) and the number of shadowing persons on a ray.

As for the influence of carrier frequency, we can find quantitative suggestions from one of our experimental results as well as from several published articles [9], [10].

Fig. 5 shows a typical result from our measurements at 900 MHz. Fig. 5(a) shows a schematic view of the measurement site. Two vertically polarized antennas with very sharp beams were placed facing each other at a distance of three meters. The antennas and the line-of-sight paths are reasonably clear of furniture and other objects to avoid any reflected or scattered rays. In the experiment, a person moved sideways along the dashed line in the figure. The height of the antennas was 150 cm and the person was 173 cm tall.

Fig. 5(b) shows the ratio of the received powers with and without human body shadowing. The horizontal axis indicates the offset position of the obstacle (i.e., the person) from the line-of-sight path. Though there is some variation of the additional loss (or gain) due to the offset position of the person, 6 dB and 90 cm (= the distance between two level crossing points at 0 dB in the vertical axis in Fig. 5) seems to be a good approximation for $L_{\rm sh}$ and $d_{\rm th}$ of the proposed model in 900-MHz band.

As for L-band, the delay profile variations with intentional shadowing reported in [9] suggest that the value for $L_{\rm sh}$ should lie between 6 and 11 dB.

Measurement results from an experiment similar to that described above in the 60-GHz band [10] show that $L_{\rm sh}$ and $d_{\rm th}$ can be set to be 18 dB and 32 cm, respectively.

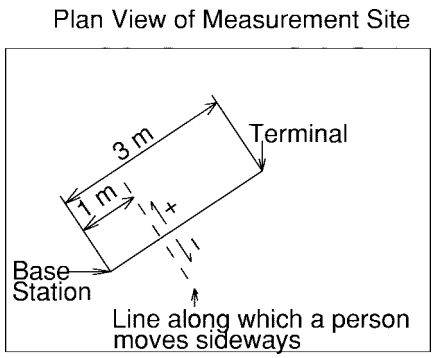

(a)

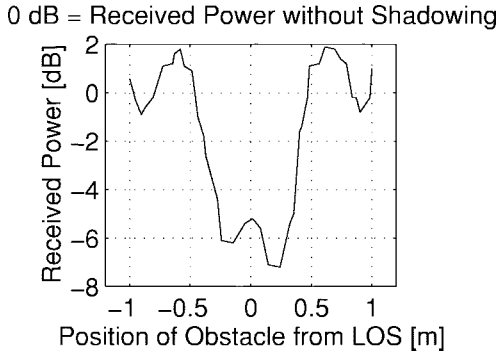

(b)

Fig. 5. A typical experimental result of human body shadowing in 900-MHz band. (a) Measurement layout. (b) The ratio of the received power compared to that without body shadowing.

In the method described in this paper, $L_{\rm sh}$ and $d_{\rm th}$ are assumed to be independent of the rest of the factors except carrier frequency.

IV. Propagation Loss Prediction Results

We apply the above model with the simple office layout already shown in Fig. 2. The imaging method is used to determine the rays, with an additional prediction of the diffracted rays [1]. A direct incoming ray and rays having two or fewer reflections/diffractions are determined. No penetrations through the walls are assumed for the moment. The propagation loss is calculated for two carrier frequencies: 900 MHz and 60 GHz. For $L_{\rm sh}$ and $d_{\rm th}$, the values obtained in Section III are used. The diffraction coefficient is calculated with the knife-edge model [16] and the reflection loss by a wall is assumed to be a constant 6 dB for approximation purpose.

Fig. 6 shows the cumulative probability of propagation loss at a line-of-sight observation point obtained by the body-shadowing model. At 900 MHz, the probability distribution is indeed concentrated around 52 dB in loss, but another small peak in probability exists around 57 dB. Considering that the outage rate of a communication link usually depends on the worst case, it is important to estimate even this smaller peak. A similar observation can be made at 60 GHz as well, while the difference in propagation loss between the two peaks is larger than that at 900 MHz.

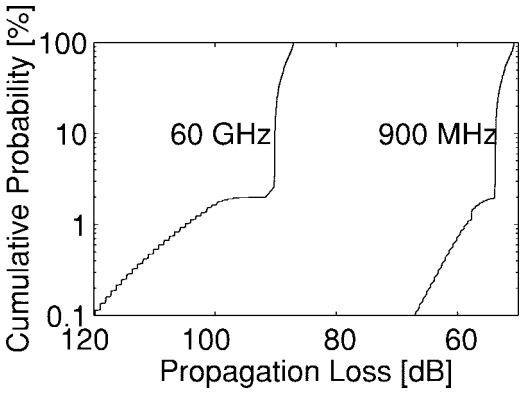

Fig. 6. Cumulative probability of propagation loss at a line-of-sight observation point at 900 MHz and 60 GHz.

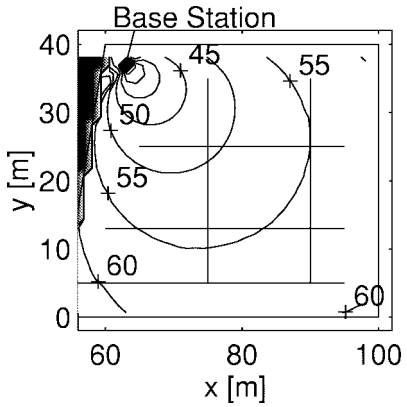

(a)

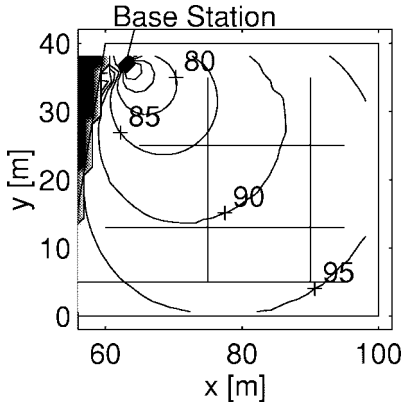

(b)

Fig. 7. Contour map (every 5 dB) of median (50% value) of propagation loss at (a) 900 MHz and (b) 60 GHz.

Figs. 7 and 8 show the difference between the median (50% value) of propagation loss and the 99% value of reliability for the given geometry. We can estimate both typical and worst-case propagation loss in the form of contour maps by using the proposed model. The contour maps (in particular, those in Fig. 8) are extremely useful to find out where coverage problems occur at the given site and where additional countermeasures against human body shadowing should be implemented.

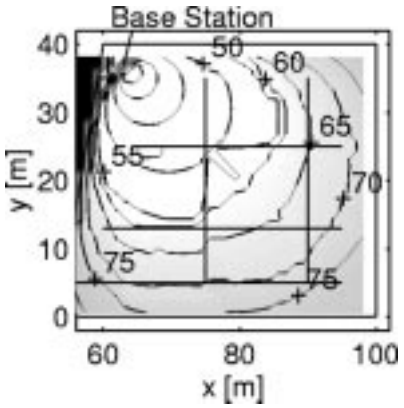

(a)

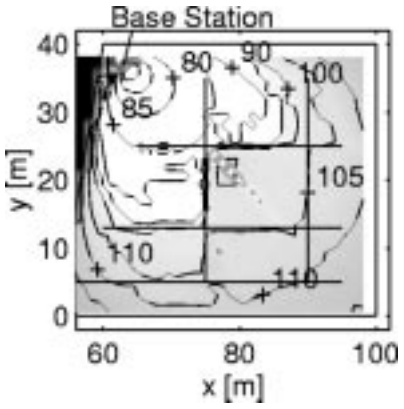

(b)

Fig. 8. Contour map (every 5 dB) of propagation loss for 99% reliability at (a) 900 MHz and (b) 60 GHz.

V. Comparison of Predicted Results with a Measurement

A measurement was performed in 900-MHz band in a typical office corridor shown in Fig. 9(a) and the result was compared with prediction by the body-shadowing model. The walkways and their shadowing probabilities shown in the figure were determined by observation with a video camera during the measurement. Note that a shadowing probability of 13% is seen at one walkway because several people spent time in front of the fax machine located near there. The directivities of the antennas used for the base station and the terminal were 12.5 and 9.0 dBi, respectively. Both antennas were vertically polarized and their half-power beam widths in horizontal plane were 65°. The data of their horizontal radiation patterns provided by the manufacturer were used in the calculation with the body-shadowing model. The antennas faced each other and their heights were 150 cm. To evaluate the local deviation, four datasets from different positions, shown in Fig. 9(b) for the terminal antenna, were collected. Each dataset was collected over a period of 15 min with a sampling interval of 0.2 s; thus, each included 4500 samples of received signal strength. The cumulative probability obtained from the 18 000 samples in the four datasets is shown in Fig. 9(c) along with the predicted results by the body-shadowing model. In the

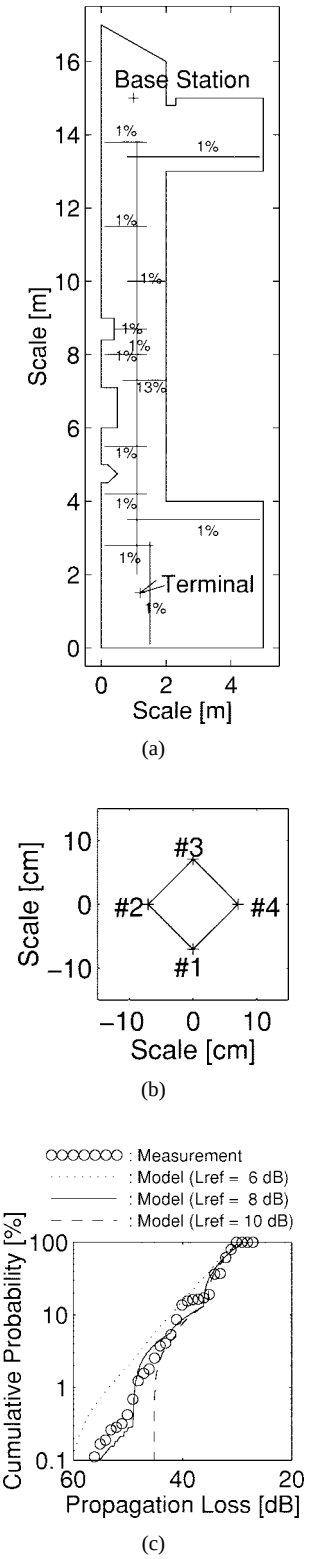

Fig. 9. Comparison with a measurement in 900-MHz band. (a) Plan view of measurement site. (b) Positions for terminal antenna. (c) Comparison of cumulative probability.

figure, the predicted results with different reflection losses by a wall $L_{\rm ref}$ are shown.

The measurement result and the prediction with $L_{\rm ref} = 8$ dB show good agreement. The differences due to $L_{\rm ref}$ of the predicted results suggest that the precise prediction of propagation loss of each incoming ray should be required to obtain a proper prediction by the body-shadowing model.

VI. Conclusion

A new statistical model for human body shadowing was proposed. The model enables us to estimate the body-shadowing effects in a specific layout of offices and factories. The model was combined with widely used propagation prediction methods based on ray tracing to yield a propagation prediction method for indoor microwave communication. The method is suitable for indoor network planning tools for indoor radio LAN. The investigation of the dependencies of $L_{\rm sh}$ and $d_{\rm th}$ on carrier frequency and other factors described in Section III is important in order to apply this body-shadowing model to various indoor radio communication systems. Further comparison with typical indoor environment measurements will be an important aspect of our future work to evaluate the prediction error of this model.

Appendix
Calculation of the Latter Part of (2)

Here we explain the case in which the shadowing events of three influential rays denoted as S_i, S_j, and S_k are not independent, which can be easily extended to the general case. The probability to obtain is $P(S_i, S_j, S_k) = P(S_i S_j S_k)$. We can generally assume

$$S_i = E_1 + E_2 + E_3 + E_5 \tag{A.1}$$
$$S_j = E_1 + E_2 + E_4 + E_6 \tag{A.2}$$
$$S_k = E_1 + E_3 + E_4 + E_7 \tag{A.3}$$

where S_i is the shadowing event for ith ray and $\{E_i\}(i = 1, 2, \cdots, 7)$ are mutually independent shadowing events.

Even when there are additional events, we can simply extend the same procedure. For example, if there are two mutually independent shadowing events for the kth ray (E_7 and E_8) and neither of them participates in the shadowing events of other rays, E_7 in the above equation can be replaced with $E_7' = E_7 + E_8$.

A way to obtain $P(S_i S_j S_k)$ is to express the product event $S_i S_j S_k$ in the form of a sum of exclusive events, which also have to be products of independent events. This is indeed possible, but the following result is rather complicated:

$$\begin{aligned} S_i S_j S_k = {} & E_1 + \overline{E_1} E_2 E_3 E_4 + \overline{E_1}\,\overline{E_2} E_3 E_4 \\ & + \overline{E_1} E_2 \overline{E_3} E_4 + \overline{E_1} E_2 E_3 \overline{E_4} \\ & + \overline{E_1}\,\overline{E_2}\,\overline{E_3} E_4 E_5 + \overline{E_1}\,\overline{E_2} E_3 \overline{E_4} E_6 \\ & + \overline{E_1} E_2 \overline{E_3}\,\overline{E_4} E_7 + \overline{E_1}\,\overline{E_2}\,\overline{E_3}\,\overline{E_4} E_5 E_6 E_7 \end{aligned} \tag{A.4}$$

and difficult to extend to the case in which four or more rays are influential.

Thus, we choose another way. We consider $2^7 = 128$ product events, namely $E_1 E_2 E_3 E_4 E_5 E_6 E_7$,

$\overline{E_1}E_2E_3E_4E_5E_6E_7, \cdots, \overline{E_1}\,\overline{E_2}\,\overline{E_3}\,\overline{E_4}\;\;\overline{E_5}\,\overline{E_6}\,\overline{E_7}$. They are mutually exclusive and the sum of all of them is the certain event I. The probability of each of them can be easily calculated like

$$\begin{aligned} &P(\overline{E_1}E_2E_3E_4E_5E_6E_7) \\ &\quad = P(\overline{E_1})P(E_2)P(E_3)P(E_4)P(E_5)P(E_6)P(E_7) \\ &\quad = (1-P(E_1))P(E_2)P(E_3)P(E_4)P(E_5)P(E_6)P(E_7) \end{aligned} \tag{A.5}$$

and $P(S_iS_jS_k)$ can be obtained as the sum of the probabilities of the events which are contained in the product event $S_iS_jS_k$. That is

$$\begin{aligned} P(S_iS_jS_k) = {} & P(E_1E_2E_3E_4E_5E_6E_7) \\ & + \cdots + P(E_1\overline{E_2}\,\overline{E_3}\,\overline{E_4}\,\overline{E_5}\,\overline{E_6}\,\overline{E_7}) \\ & + P(\overline{E_1}E_2E_3E_4E_5E_6E_7) \\ & + \cdots + P(\overline{E_1}E_2E_3E_4\overline{E_5}\,\overline{E_6}\,\overline{E_7}) \\ & + P(\overline{E_1}\,\overline{E_2}E_3E_4E_5E_6E_7) \\ & + \cdots + P(\overline{E_1}\,\overline{E_2}E_3E_4\overline{E_5}\,\overline{E_6}\,\overline{E_7}) \\ & + P(\overline{E_1}E_2\overline{E_3}E_4E_5E_6E_7) \\ & + \cdots + P(\overline{E_1}E_2\overline{E_3}E_4\overline{E_5}\,\overline{E_6}\,\overline{E_7}) \\ & + P(\overline{E_1}E_2E_3\overline{E_4}E_5E_6E_7) \\ & + \cdots + P(\overline{E_1}E_2E_3\overline{E_4}\,\overline{E_5}\,\overline{E_6}\,\overline{E_7}) \\ & + P(\overline{E_1}\,\overline{E_2}\,\overline{E_3}E_4E_5E_6E_7) \\ & + \cdots + P(\overline{E_1}\,\overline{E_2}\,\overline{E_3}E_4E_5\overline{E_6}\,\overline{E_7}) \\ & + P(\overline{E_1}\,\overline{E_2}E_3\overline{E_4}E_5E_6E_7) \\ & + P(\overline{E_1}\,\overline{E_2}E_3\overline{E_4}E_5E_6\overline{E_7}) \\ & + P(\overline{E_1}\,\overline{E_2}E_3\overline{E_4}\,\overline{E_5}E_6E_7) \\ & + P(\overline{E_1}\,\overline{E_2}E_3\overline{E_4}\,\overline{E_5}E_6\overline{E_7}) \\ & + P(\overline{E_1}E_2\overline{E_3}\,\overline{E_4}E_5E_6E_7) \\ & + P(\overline{E_1}E_2\overline{E_3}\,\overline{E_4}E_5E_6\overline{E_7}) \\ & + P(\overline{E_1}E_2\overline{E_3}\,\overline{E_4}\,\overline{E_5}E_6E_7) \\ & + P(\overline{E_1}E_2\overline{E_3}\,\overline{E_4}\,\overline{E_5}\,\overline{E_6}E_7) \\ & + P(\overline{E_1}\,\overline{E_2}\,\overline{E_3}\,\overline{E_4}E_5E_6E_7). \end{aligned} \tag{A.6}$$

At first glance, this way seems more difficult than the first one. But, to complete Step 1 we have to calculate not only $P(S_1S_2S_3)$, but also $P(\overline{S_1}S_2S_3), \cdots, P(\overline{S_1}\,\overline{S_2}\,\overline{S_3})$ and each of the 128 events is contained in one of the above eight product events, i.e.,

$$\begin{aligned} P(\overline{S_i}S_jS_k) = {} & P(\overline{E_1}\,\overline{E_2}\,\overline{E_3}E_4\overline{E_5}E_6E_7) \\ & + P(\overline{E_1}\,\overline{E_2}\,\overline{E_3}E_4\overline{E_5}E_6\overline{E_7}) \\ & + P(\overline{E_1}\,\overline{E_2}\,\overline{E_3}E_4\overline{E_5}\,\overline{E_6}E_7) \\ & + P(\overline{E_1}\,\overline{E_2}\,\overline{E_3}E_4\overline{E_5}\,\overline{E_6}\,\overline{E_7}) \\ & + P(\overline{E_1}\,\overline{E_2}\,\overline{E_3}\,\overline{E_4}\,\overline{E_5}E_6E_7) \end{aligned} \tag{A.7}$$

$$P(\overline{S_i}\,\overline{S_j}S_k) = P(\overline{E_1}\,\overline{E_2}\,\overline{E_3}\,\overline{E_4}\,\overline{E_5}\,\overline{E_6}E_7) \tag{A.8}$$

$$P(\overline{S_i}\,\overline{S_j}\,\overline{S_k}) = P(\overline{E_1}\,\overline{E_2}\,\overline{E_3}\,\overline{E_4}\,\overline{E_5}\,\overline{E_6}\,\overline{E_7}). \tag{A.9}$$

Thus, all of the 128 events should be calculated in any case to complete the step. To examine which out of the eight events includes each product event out of 128, an ordinary logical calculation by bit flags can be used.

Most of the computation time for the calculation is devoted to the multiplications of the probabilities of the 128 events. In general, when the number of the rays is N and the shadowing events of M rays out of N are independent of the shadowing events of any other rays, the number of the product events that should be calculated such as the above $E_1E_2E_3E_4E_5E_6E_7$ is

$$2^{2^{N-M}-1}. \tag{A.10}$$

Thus, the count of multiplications is

$$((2^{N-M}-1)-1) \times 2^{2^{N-M}-1}. \tag{A.11}$$

ACKNOWLEDGMENT

The authors would like to thank the members of the Radio Communication Systems Group, Department of Signals, Sensors, and Systems, Royal Institute of Technology, Sweden, for valuable discussions and suggestions. They would also like to thank J.-E. Berg and his colleagues of Ericsson Radio Systems AB, Sweden, for their support of the measurement.

REFERENCES

[1] J. W. McKnown and R. L. Hamilton, Jr., "Ray tracing as a design tool for radio networks," *IEEE Network Mag.*, vol. 5, pp. 27–30, Nov. 1991.
[2] S. Takahashi, K. Ishida, H. Yoshiura, and A. Nakagoshi, "An evaluation point culling algorithm for radio propagation simulation based on the imaging method," in *Proc. Virginia Tech 5th Symp. Wireless Personal Commun.*, Blacksburg, VA, p. 13, June 1995.
[3] S. Y. Seidel and T. S. Rappaport, "A ray tracing technique to predict path loss and delay spread inside buildings," in *Conf. Rec. IEEE GLOBECOM*, Orlando, FL, Dec. 1992, pp. 649–653.
[4] S. J. Fortune, D. M. Gay, B. W. Kernighan, O. Landron, R. A. Valenzuela, and M. H. Wright, "WISE design of indoor wireless systems: Practical computation and optimization," *IEEE Computat. Sci. Eng.*, vol. 2, no. 1, pp. 58–68, Spring 1995.
[5] P. Kreuzgruber, P. Unterberger, and R. Gahleitner, "A ray splitting model for indoor radio propagation associated with complex geometries," in *43rd IEEE Veh. Technol. Conf.*, Secaucus, NJ, May 1993, pp. 227–230.
[6] R. J. C. Bultitude, "Measurement, characterization and modeling of indoor 800/900 MHz radio channels for digital communications," *IEEE Communicat. Mag.*, vol. 25, pp. 5–12, June 1987.
[7] J. A. Roberts and J. R. Abeysinghe, "A two-state Rician model for predicting indoor wireless communication performance," in *Proc. IEEE Int. Conf. Communicat*, Seattle, WA, June 1995, pp. 40–43.
[8] Y. Kanada, "The influence of a moving obstacle upon indoor radio propagation," in *Proc. Inst. Electron., Inform., Commun. Eng. Fall Conf.*, Sapporo, Japan, Sept. 1993, pp. 2–19 (in Japanese).
[9] S. Obayashi and T. Maeda, "Time variation of the magnitude and phase of multipath delay in practical indoor radio channels," in *Inst. Elect. Eng. Conf. Antennas Propagat.*, York, U.K., pp. 488–491, Apr. 1991.
[10] K. Sato, H. Masuzawa, T. Manabe, and T. Ihara, "Measurements of shadowing due to human body at 60 GHz," in *Proc. Inst. Electron., Inform., Commun. Eng. Spring Conf.*, Yokohama, Japan, Mar. 1994, p. B-15 (in Japanese).
[11] F. Ikegami, S. Yoshida, T. Takeuchi, and M. Umehira, "Propagation factors controlling mean field strength on urban street," *IEEE Trans. Antennas Propagat.*, vol. AP-32, pp. 822–829, Aug. 1984.
[12] J. D. Parsons, *The Mobile Radio Propagation Channel*. London, U.K.: Pentech, 1992, pp. 110–113.
[13] W. C. Y. Lee, *Mobile Communications Engineering*. New York: McGraw-Hill, 1985, p. 30.
[14] A. Papoulis, *Probability, Random Variables, and Stochastic Processes*, 2nd ed. New York: McGraw-Hill, 1984, pp. 119–120.
[15] J. D. Parsons, *The Mobile Radio Propagation Channel*. London, U.K.: Pentech, 1992, pp. 134–135.
[16] W. C. Y. Lee, *Mobile Communications Engineering*. New York: McGraw-Hill, 1985, pp. 122–124.

Shuichi Obayashi (M'91) was born in Kawanishi, Hyogo, Japan, in 1962. He received the B.E. and M.E. degrees from Kyoto University, Kyoto, Japan, in 1985 and 1987, respectively.

He joined the Toshiba Corporation, Kawasaki, Japan, in 1987. From 1995 to 1996 he was a Guest Researcher of the Royal Institute of Technology (KTH), Stockholm, Sweden. His current research and development interests are in the area of indoor and mobile radio propagation, antenna arrays, mobile communication terminal, and RF/microwave components.

Mr. Obayashi is a member of the IEICE of Japan and received the Young Engineer Award from that institute in 1995.

Jens Zander (S'82–M'85) received the M.S. (electrical engineering) and Ph.D degrees from Linköping University, Sweden, in 1979 and 1985, respectively.

From 1985 to 1989, he was a Partner and Vice President of SECTRA, Sweden, a research and development consultant firm. In 1989 he was appointed Professor and Head of the Radio Communication Systems Laboratory, Royal Institute of Technology, Stockholm, Sweden. Since 1992, he has also served as Senior Scientific Advisor (Associate Research Manager) to the Swedish National Deference Research Establishment and a board member of TERACOM, the Swedish National broadcasting operator. In addition, he serves as consultant to government agencies and industry on spectrum allocation issues. He has published numerous papers in the field of radio communication, in particular, on the aspects of spectrum resource management for personal communication systems. He has published three textbooks in radio communication systems. His current research interests include the economics and resource allocation issues in future multimedia wireless infrastructures, systems for digital wireless broadcasting, and autonomous tactical communication systems.

Dr. Zander was the recipient of the IEEE Vehicular Technology Society Jack Neubauer Award for Best Systems Paper in 1992. He is an adjoint member of the Swedish URSI Committee (sections C and G/H).